The phenomena of spin-filter tunnelling

2007 J. Phys.: Condens. Matter 19 165202

(http://iopscience.iop.org/0953-8984/19/16/165202)

IOP PUBLISHING JOURNAL OF PHYSICS: CONDENSED MATTER

J. Phys.: Condens. Matter **19** (2007) 165202 (24pp) doi:10.1088/0953-8984/19/16/165202

The phenomena of spin-filter tunnelling

Jagadeesh S Moodera[1], **Tiffany S Santos**[1] **and Taro Nagahama**[1,2]

[1] Francis Bitter Magnet Laboratory, Massachusetts Institute of Technology, Cambridge, MA 02139, USA
[2] National Institute of Advanced Industrial Science and Technology (AIST), NanoElectronics Research Institute, Tsukuba, Ibaraki 305-8568, Japan

Received 22 September 2006
Published 6 April 2007
Online at stacks.iop.org/JPhysCM/19/165202

Abstract

The spin filtering phenomenon allows one to obtain highly spin-polarized charge carriers generated from nonmagnetic electrodes using magnetic tunnel barriers. The exponential dependence of tunnel current on the tunnel barrier height is operative here. The magnetic, semiconducting europium chalcogenide compounds have strikingly demonstrated this effect. The possibility of employing ferrites and other methods opens the potential for display of this phenomenon at room temperature, which can be expected to lead to huge progress in spin injection and detection in semiconductors. But first, extremely challenging material-related issues have to be addressed. This review covers the field.

(Some figures in this article are in colour only in the electronic version)

1. Spin-polarized tunnelling introduction

The phenomenon of tunnelling is a direct consequence of quantum mechanics, which has been described recently [1]. Although the concept existed in the late 1920s, the field developed rapidly since the classic experiments of the tunnel current between a superconductor and a normal metal through a thin Al_2O_3 barrier by Giaever [2]. Immediately following, there was huge activity in experimental and theoretical research in tunnelling, starting with superconductivity and later encompassing a broader field.

The BCS theory of superconductivity describes the superconducting current carriers as pairs of electrons in time-reversed states $(+k\uparrow, -k\downarrow)$ with not only opposite momenta, but also opposite spins [3]. The dramatic increase of the orbital parallel critical field of superconducting Al films from about 100 G to 5 T as they are made thinner, together with an increase in the superconducting transition temperature from 1.1 K to about 2.5 K, were essential for the original spin polarization measurements. One of the remarkable tunnelling experiments was the observation of the spin splitting of the quasiparticle states in a tunnelling measurement [4], as shown in figure 1 for a $Al/Al_2O_3/Ag$ tunnel junction, where Ag is a normal metal and the superconducting Al film is 4 nm thick.

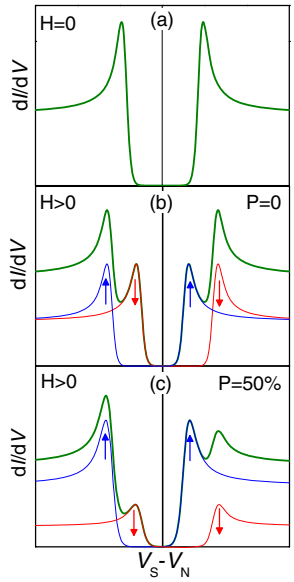

Figure 1. (a) Conductance ($\mathrm{d}I/\mathrm{d}V$) versus bias at zero field for a superconductor/insulator/metal tunnel junction. The superconducting energy gap is centred at $V = 0$. There are two peaks at finite bias, corresponding to the quasiparticle DOS. (b) $\mathrm{d}I/\mathrm{d}V$ in an applied field, showing Zeeman splitting of the DOS. The deconvolved spin-up (blue/dashed) and spin-down (red/dotted) DOSs are shown, as well as the resulting measured curve (green/solid), which is completely symmetric when $P = 0$, for a nonmagnetic metal counter electrode. (c) $\mathrm{d}I/\mathrm{d}V$ in an applied field with $P = 50$, when the counter electrode is a ferromagnet. The spin-up DOS is greater than the spin-down DOS, resulting in an asymmetric curve.

The spin splitting of the superconducting density of states (DOS) in Al led to the phenomenal first spin-polarized tunnelling (SPT) experiment by Meservey and Tedrow [5]: the superconducting Al acting as a spin detector for the tunnelling electrons from a ferromagnet (FM) counter-electrode in $\mathrm{Al/Al_2O_3/FM}$. Conservation of electron spin in the tunnelling process is important in the observation of spin polarization. Several excellent reviews have been written on the subject over the years [6–9]. The spin polarization P is defined as

$$P = [N_\uparrow(E_\mathrm{F}) - N_\downarrow(E_\mathrm{F})]/[N_\uparrow(E_\mathrm{F}) + N_\downarrow(E_\mathrm{F})] \tag{1}$$

where $N_\uparrow(E_\mathrm{F})$ and $N_\downarrow(E_\mathrm{F})$ are the number of majority spin and minority spin electrons in the tunnelling current near the Fermi energy E_F.

Looking at the curves in figure 1, the conductance as a function of bias shows the superconducting energy gap of Al film (a). The Zeeman splitting seen in (b) is the spin-split BCS density of states of the superconducting Al thin film in a parallel magnetic field, in which the orbital screening currents and spin–orbit scattering are negligible. Here the quasiparticle states with magnetic moments parallel to the magnetic field are at lower energy $-\mu_\mathrm{B}H$ and those that are antiparallel to the field move to higher energy $+\mu_\mathrm{B}H$. This technique of producing almost pure spin-polarized tunnel currents of either spin direction from superconducting Al films was successfully applied to measure the apparent spin sub-band densities of states of the 3d ferromagnets. That is, when the counter-electrode is a ferromagnet, as in (c), the unequal densities of spin-up and spin-down electron states introduce an additional asymmetry in the conductance curves. Such a conductance curve shown in (c) is fitted to Maki–Fulde [10] theory to derive the spin polarization of the ferromagnet. This is the basis of SPT in a tunnel junction comprising a ferromagnetic counter-electrode.

In all the measurements with a Al_2O_3 barrier, positive P was seen. The positive sign indicated that the tunnelling electrons had predominantly majority spin, $N_\uparrow > N_\downarrow$. In SPT measurements the spin polarization comes from the spin-polarized itinerant electrons of the ferromagnet that take part in tunnelling [11], assuming (as had Bardeen [12] with superconductors) that the matrix elements determining the tunnelling probability are independent of spin, led to predicted values for the polarizations, which agreed with earlier measured values which were slightly low especially for Ni. However, with cleaner interfaces the revised values [7, 9] for the polarizations are $P_{Ni} = 46\%$, $P_{Co} = 42\%$, and $P_{Fe} = 45\%$. The true definition of P in tunnelling has been well described by Mazin [13], wherein it is said that the DOS should be weighted by the Fermi velocity squared for the two spin directions when dealing with transport spin polarization. For example, $N_{\uparrow,\downarrow}(E_F)$ is replaced by $\langle N\upsilon^2\rangle_{\uparrow,\downarrow}$, where υ is the Fermi velocity and N is the DOS at the Fermi level. In other words, the Stearns model and subsequent models [14] note that, although most of the d electrons are highly localized, one of the d bands in Ni and in Fe, which crosses the Fermi surface, is nearly parabolic and has an effective mass close to that of a free electron. These highly mobile 'itinerant d electrons' (which resulted from s–d hybridization and were designated d_i electrons by Stearns) are assumed to dominate the tunnel current [11, 13, 15].

In the traditional SPT measurements, the junctions were made by depositing an ultrathin layer of metallic Al, and oxidizing some of it to create an Al_2O_3 insulating barrier; this is followed by a ferromagnetic counter-electrode deposition. Using a superconducting film with its spin-splitting is by far the most unambiguous method of measuring the spin polarization of the tunnel current because of the long coherence length of superconductors. There is good understanding of the theory and experimental method of superconducting tunnel spectroscopy. Tunnelling between magnetic materials can also be applied to measure P (where one FM with well defined P acts as the spin detector) as it has the advantage that it can be performed at room temperature in a small applied magnetic field [7]. However, because of the very short coherence length of ferromagnetism in metals, the effect of the metal surface and the interface with the tunnel barrier must be well controlled down to a monolayer level to obtain reproducible results.

With amorphous Al_2O_3 as the tunnel barrier, in the case of transition metals and alloys the highest measured value of P is ∼52%, for CoFe alloy [16]. Interestingly, one can expect higher P values for half-metallic ferromagnets, which are predicted to have only one spin band crossing E_F whereas they have an energy gap for the other spin orientation, thus leading to completely spin-polarized conduction electrons [17–19]. For example, some of the candidate materials that fall into this category are NiMnSb, CrO_2, $La_{1-x}Sr_xMnO_3$ etc, and among them only CrO_2 has shown $P \approx 100\%$ by SPT measurements [20]. The half-metallicity is extremely dependent on the careful control of stoichiometry (with site specificity as well) and structure of the compounds. The major difficulties in seeing 100% polarized tunnelling electrons by this approach lies in making these compounds stable, stoichiometric and maintaining half-metallicity to the last atomic layer at the interface (including bonding with the barrier atoms/molecules which can also change its behaviour) is nontrivial and extremely challenging [21, 22].

In the original SPT work using a tunnel device of the structure, $Al/Al_2O_3/FM$, the observed polarization of the tunnel current appears from the spin imbalance of the DOS of spin-up and spin-down conduction electrons at the Fermi energy in the ferromagnetic electrode, the highest being about 52% with transition metal alloys. However, even higher values of P can be obtained by using spin selective barriers that have a different tunnelling probability $|T|^2$ for the two spin directions: $|T\uparrow|^2 > |T\downarrow|^2$. For instance, one such barrier material is the ferromagnetic semiconductor EuS, having a band gap of 1.65 eV and a ferromagnetic Curie temperature of $T_C = 16.6$ K. In the ferromagnetic state the exchange splitting of the conduction

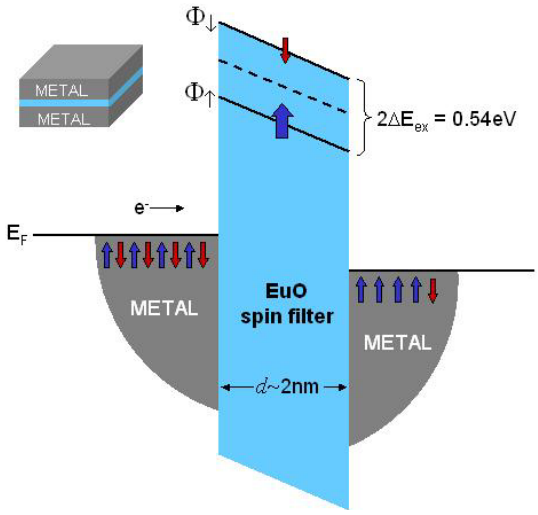

Figure 2. Schematic diagram of the tunnelling spin-filter effect in a metal/EuO spin filter/metal tunnel junction. Electrons with randomly oriented spins tunnel from the Fermi level of the nonmagnetic metal through the EuO spin-filter barrier. The spin-split conduction band of ferromagnetic EuO creates a lower barrier height for spin-up electrons ($\Phi_\uparrow$) and higher barrier height for spin-down electrons ($\Phi_\downarrow$), giving rise to a highly spin-polarized current.

band is $2\Delta E_{\rm ex}$, leading to two barrier heights of $\Phi_{\downarrow,\uparrow} = \Phi_0 \pm \Delta E_{\rm ex}$ for spin-down and spin-up electrons, where Φ_0 is the average barrier height at a temperature above $T_{\rm C}$. Since the tunnelling probability varies exponentially with barrier height, the spin-up current can greatly exceed the spin-down current, yielding spin-polarized current in a nonmagnetic metal/EuS/nonmagnetic metal tunnel junction. In this review we deal with this phenomenon as presented below.

2. Filtering spins

In contrast to conventional SPT devices using a ferromagnetic metal as the source for spin-polarized electrons, in the novel approach of spin-filter tunnelling a ferromagnetic *tunnel barrier* is used to generate a polarized current, called the spin-filter effect, shown schematically in figure 2. In such a ferromagnetic semiconducting barrier, in the magnetically ordered state, exchange splitting of the conduction band creates two different tunnel barrier heights, a lower one for spin-up electrons ($\Phi_\uparrow$) and a higher one for spin-down electrons ($\Phi_\downarrow$). In general, during the tunnelling process spin is conserved [6]. Therefore, for a given barrier thickness, the tunnel current density J depends exponentially on the corresponding barrier heights [23, 24]:

$$J_{\uparrow(\downarrow)} \propto \exp(-\Phi_{\uparrow(\downarrow)}^{1/2} d). \tag{2}$$

Therefore, even with a modest difference in barrier heights, the tunnel probability for spin-up electrons is much greater than that for spin-down electrons, resulting in spin polarization (P) of the tunnel current:

$$P = \frac{J_\uparrow - J_\downarrow}{J_\uparrow + J_\downarrow}. \tag{3}$$

The magnitude of exchange splitting ($2\Delta E_{\rm ex}$) for spin-filter materials such as the europium chalcogenides is substantial; for example, the largest is 0.54 eV for EuO, which could completely filter out spin-down electrons, leading to $P = 100\%$.

Table 1. Spin-filter materials.

Material	Magnetic behaviour	T_C (K)	Moment (μ_B)	Structure, a (nm)	E_g (eV)	$2\Delta E_{ex}$ (eV)	P (%)	Spin-filter reference
EuO	FM	69.3	7.9	Fcc, 0.514	1.12	0.54	29	Santos and Moodera [27]
EuS	FM	16.6	7.9	Fcc, 0.596	1.65	0.36	86	Moodera [25]
EuSe	AFM	4.6	7.9	Fcc, 0.619	1.80		100	Moodera [26]
$BiMnO_3$	FM	105	3.6	Perovskite			22	Gajek [30]
$NiFe_2O_4$	Ferri-M	850	2	Spinel	1.2		22	Lüders [31]
$CoFe_2O_4$	Ferri-M	796	3	Spinel	0.57			

The spin-filter effect has been well observed in europium chalcogenide tunnel barriers EuS [25] and EuSe [26] and more recently with EuO [27]: EuS barriers have shown P as high as 85% even at zero applied magnetic field. Interestingly, in the case of EuSe, which is an antiferromagnet that becomes ferromagnetic in a small applied magnetic field, field-dependent exchange splitting of the conduction band appears. Due to this, the resulting P turns out to be field dependent in the case of EuSe barriers: $P = 0$ in zero field and increases with applied field, reaching nearly 100% at 1 T. EuS and EuSe have magnetic ordering temperatures of 16.6 K (ferromagnetic) and 4.6 K (antiferromagnetic), respectively, and thus only filter spins at temperatures in the liquid helium temperature range.

With a higher T_C, 69.3 K, and greater exchange splitting, EuO holds promise to reach greater spin-filter efficiency at higher temperatures. Furthermore, the T_C of EuO can be raised well above liquid nitrogen temperatures, even to ∼170 K, by doping with rare-earth metals (discussed later), although doping has shown the lowering of $2\Delta E_{ex}$. The T_C of EuS can also be raised by extrinsic doping or by making Eu-rich EuS [28], but still remains well below the T_C of EuO. However, demonstrating the spin-filter effect in EuO is a more challenging task than with EuS and EuSe. The difficulty lies in obtaining high quality, stoichiometric, ultrathin EuO films. Good quality ultrathin films of EuS and EuSe are easily evaporated directly from a powder source of EuS and EuSe. While powder sources of the more stable nonmagnetic Eu_2O_3 are readily available, EuO (the metastable oxide form) is not available, and is therefore much more difficult to make as an ultrathin film needed for a tunnel barrier.

The europium chalcogenides are not the only candidates for spin-filter materials. There has been some progress recently with other promising candidates, namely ferrites and perovskites. Ferrites have magnetic ordering temperatures well above room temperature and thus could potentially filter spins at a convenient temperature range. However, with their complex structure, the materials aspects are complicated. Experiments showing spin filtering in ferrimagnetic, insulating $NiFe_2O_4$ will be described later. Ferrimagnetic $CoFe_2O_4$ is another candidate material [29], and experiments showing direct evidence of spin filtering in $CoFe_2O_4$ are being developed. Among the perovskites, some degree of spin filtering has been observed using insulating, ferromagnetic $BiMnO_3$ with a T_C of 105 K. Table 1 lists the properties of the known spin-filter materials.

3. Electronic structure of Eu chalcogenides

The interesting magnetic, optical and electronic properties of the europium chalcogenides in bulk, crystalline form and thick film form were extensively characterized in the 1960s

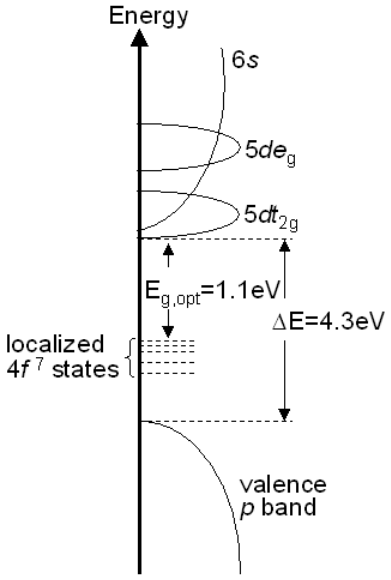

Figure 3. Energy level diagram of EuO, which is representative of the europium chalcogenides [32–34].

and 1970s. For a review of this early work, see [32–35]. The following section covers properties that are relevant for the discussion of these materials as spin filters. The europium chalcogenides are ideal Heisenberg ferromagnets with a large theoretical effective magnetic moment $\mu_B g\sqrt{J(J+1)} = 7.9\ \mu_B$ which has been closely matched experimentally in bulk single crystals and thin films, though band structure calculations [36–38] predict a moment between 6.8 and 7 μ_B. The electronic structure of, for example, EuO (shown schematically in figure 3) and the magnitude of the exchange splitting of the conduction band were first determined in optical studies by Wachter *et al* [33]. The magnetic moment originates from the half-filled $4f^7$ states, which are localized within the energy gap between the valence band and the conduction band. The energy gap between these $4f^7$ states and the $5dt_{2g}$ states at the bottom of the conduction band defines the optical band gap (E_g).

For $T > T_C$, the conduction band is unpolarized. As EuO is cooled below the T_C, ferromagnetic ordering of the $4f^7$ states causes the conduction band to split into two energy levels, one lowered in energy by an amount ΔE_{ex} and the other raised by ΔE_{ex}. The spin degeneracy is lifted—up-spins occupy the lower energy level and down-spins occupy the higher energy level. This exchange splitting of the conduction band causes a reduction in E_g between the $4f^7$ states and the conduction band, which is observed optically by a red shift of the absorption edge. The exchange interaction H_{exch} is given by the following Heisenberg exchange relation: $H_{exch} = 2\Delta E_{ex} = -2J_C\Sigma\vec{s}\cdot\vec{S}$, where $\vec{s}$ is the spin of a conduction electron, $\vec{S}$ is the spin of neighbouring Eu^{2+} ions and J_C is the space-dependent exchange constant between the ion spin and the electron spin. Busch *et al* [39] were the first to determine the magnitude of the exchange splitting by measuring the red shift of the absorption edge (shift of the optical band gap to lower energy) in single-crystal samples upon cooling below T_C. They found $2\Delta E_{ex} = 0.54$ eV for EuO. Exchange splitting of the conduction band was reported again recently using spin-resolved x-ray absorption spectroscopy [40]. A thin film of Eu-rich EuO consisting of doped n-type carriers was used in this study. They concluded that the doped carriers in the exchange-split conduction band are 100% spin polarized, forming a half-metal.

3.1. Effect of doping

As mentioned earlier, the T_C of EuO can be raised significantly by doping with rare-earth metals Gd, La, and Ho [41]. These dopants are substitutional, replacing the Eu^{2+} ion with a trivalent ion, thus creating free electrons. T_C as high as ∼170 K was found in a recent study of 4% Gd-doped EuO thin films [42]. Eu-rich EuO films, with a high concentration of inhomogeneously dispersed oxygen vacancies, have also been found to have an enhanced T_C as high as 148 K [43]. Earlier, Schoenes and Wachter [44] extensively studied the effects of n-type Gd doping on the magneto-optical properties of EuO, and found that T_C increased with increasing carrier concentration N_e, whereas H_{exch} decreased with N_e. According to a theory by Kasuya and Yanase [45], impurity electrons stay in the vicinity of the donor and magnetically polarize neighbouring Eu^{2+} spins, creating an additional exchange interaction. Thus, the presence of an impurity electron effectively creates what Kasuya and Yanase termed a giant spin molecule, which results in a higher T_C. However, because the exchange interaction of the impurity electrons decreases with increasing N_e (observed experimentally as a decrease in magnitude of the red shift (ΔE_{ex}) with increasing N_e), the T_C reaches a maximum at a certain dopant concentration.

4. Early evidence of spin filtering

The first demonstration of high spin polarization resulting from the spin-filter effect in EuS was by Müller *et al* [46]. Field-emitted electrons from tungsten tips coated with EuS were found to have a spin polarization of $89 \pm 7\%$ at low temperature. Similar work later confirmed that electrons tunnel from the Fermi level of the tungsten into the exchange-split EuS conduction band [47–49]. The high spin polarization of the emitted electrons results from the different potential barriers for spin-up and spin-down electrons at the W–EuS interface. This is direct evidence of spin filtering in EuS.

5. Spin-filter tunnelling: EuS, EuSe and EuO tunnel barriers

The early work of Esaki *et al* [50], performed previous to the field-emission experiments, utilized EuS and EuSe films, between 20 and 60 nm thick, sandwiched between either Al or Au electrodes. With this structure they observed tunnelling across the potential barrier between the metal and the Eu chalcogenide, as shown in figure 4(a). This potential barrier is formed by the energy difference between the Fermi level of the metal electrode and the bottom of the conduction band in the Eu chalcogenide. When measuring the temperature dependence of the I–V behaviour of these junctions, a significant drop in voltage (measured with constant current) occurred below the T_C for both EuS and EuSe junctions, shown in figure 4(b). This drop results from the exchange splitting of the conduction band thereby lowering the barrier height. The application of a magnetic field causes a bigger drop at temperatures slightly higher than the T_C, shown in figure 4(b) for EuSe. However, the 20% decrease in R_J below ∼10 K at $H = 0$ for EuSe is surprising given the fact that it is an antiferromagnet at zero field and thus no exchange splitting is expected (see the discussion for EuSe below). Spin polarization of the current was not quantified in this early tunnelling experiment, whereas it showed indirect evidence of spin-filter tunnelling. Similar behaviour of junction resistance can be seen for all Eu chalcogenide junctions described later. A few years after Esaki's work, Thompson *et al* [51] also measured an increase in conductance at low temperatures due to conduction band splitting in a Schottky barrier made from a EuS single crystal and an indium metal contact.

Subsequently, spin-filtering properties of Eu chalcogenide tunnel barriers have been shown by direct measurement of spin polarization via the Meservey–Tedrow technique, whereby a

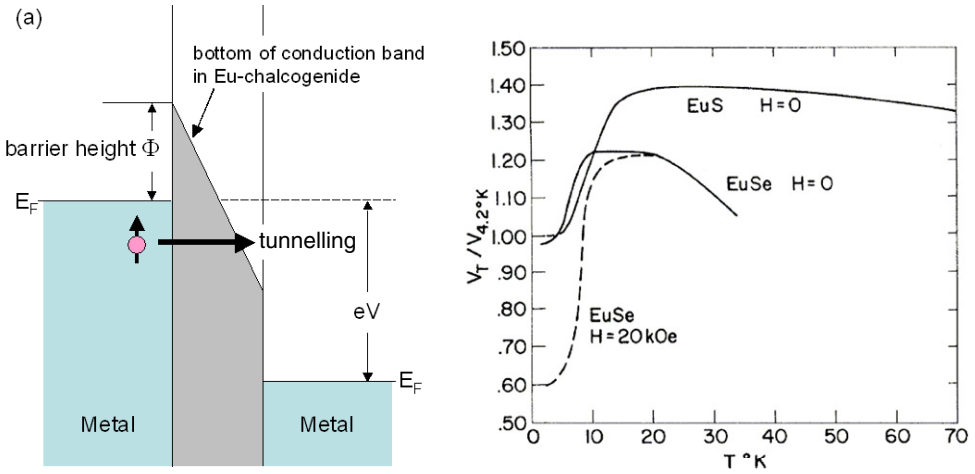

Figure 4. (a) Energy diagram for metal/EuS or EuSe/metal junction of Esaki *et al*. Φ is the barrier height for tunnelling from the metal into the bottom of the conduction band of EuS or EuSe. (b) Normalized voltage across the junction (measured with constant current) versus temperature, with and without applying a magnetic field. Figure from [50].

superconducting Al electrode was used to detect the spin of the tunnelling electrons. This will be described in more detail in the following sections. Tunnel junctions for these studies were made *in situ* in a high vacuum chamber on glass substrates, with the general structure Al/EuX/M (where M = Al or Au or Ag). EuS and EuSe tunnel barriers (about 1–4 nm thick) were deposited by thermal evaporation from EuS and EuSe powder sources, whereas EuO was grown by reactive evaporation of Eu metal in the presence of a small amount of oxygen flow. The metal electrodes were deposited by thermal evaporation and patterned by shadow masks into a cross configuration. The Al electrode deposited on a liquid nitrogen-cooled substrate was typically 4.2 nm thick. Conductance was measured at 0.4 K, well below the critical temperature of the Al superconducting electrode (∼2.5 K), similar to the case of SPT measurements. The degree of spin polarization of the tunnel current was calculated from the measured dynamic tunnel conductance ($\mathrm{d}I/\mathrm{d}V$) within a few millivolts of the Fermi level.

5.1. EuS

The initial demonstration of spin-filter tunnelling by SPT was performed using a ferromagnetic EuS barrier [25]. Dynamic tunnel conductance versus voltage at 0.4 K for a Au/EuS/Al tunnel junction is shown in figure 5 for various small applied magnetic fields (H_{appl}). In comparison, the $\mathrm{d}I/\mathrm{d}V$ curve at zero applied field for a junction with a nonferromagnetic barrier (i.e. Al_2O_3) is completely symmetric, with two peaks showing the superconducting (SC) energy gap in Al (see for example figure 1(a)). The *zero-field conductance* for the EuS junction is *asymmetric* with *four* peaks (similar to figure 1(c)). These four peaks, corresponding to the Zeeman splitting of the Al quasiparticle DOS, are more pronounced at 0.07 T. Asymmetry of these spin-split peaks is the signature of the spin-polarized tunnel current. To extract the polarization value, these $\mathrm{d}I/\mathrm{d}V$ curves were fitted using Maki's theory [10] for a thin film superconductor in a magnetic field, yielding a large value of $P = 80 \pm 5\%$.

The magnitude of Zeeman splitting is equal to $2\ \mu_{\mathrm{B}} H_0$, where μ_{B} is the Bohr magneton and H_0 is the magnetic field. Interestingly, the amount of Zeeman splitting in the $\mathrm{d}I/\mathrm{d}V$

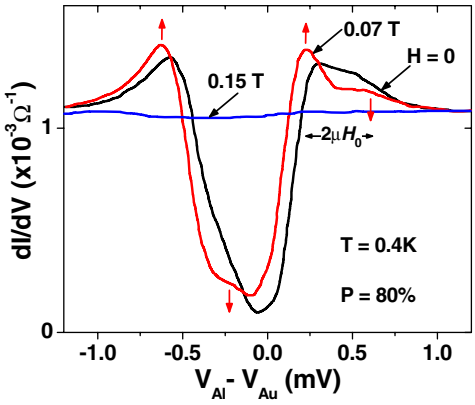

Figure 5. Dynamic conductance versus voltage of a Au/EuS/Al junction at 0.4 K in the indicated applied magnetic field. Fit of the curves to Maki's theory gives $P = 80 \pm 5\%$. The arrows indicate the spin of the Zeeman-split DOS for the 0.07 T curve. The amount of Zeeman splitting ($2\ \mu_B H_0$) is indicated for the 0.07 T curve.

measurement at $H_{appl} = 0.07$ T actually corresponds to a much higher effective field of $H_0 = 3.46$ T. The internal exchange field of the ordered ferromagnetic Eu^{2+} ions in the EuS barrier, acting on the quasiparticles of the superconducting Al (discussed in detail later), causes this phenomenally enhanced Zeeman splitting. This additional field was shown not to be an effect of the EuS fringing field, as its saturation magnetization $4\pi M_0 \sim 1.5$ T. This internal field is even large enough to drive the Al normal at $H_{appl} = 0.15$ T, as seen in figure 5, which otherwise occurs at ∼5 T for nonferromagnetic Al_2O_3 barriers. Zeeman splitting and polarization was observed even at zero applied field, showing that there is significant remanent magnetization in the EuS ultrathin layer. Though the magnitude of the internal field depends on the applied field (field needed to magnetically align and saturate EuS), the same $P = 80\%$ persists even at zero applied field. Because the *electrodes are not ferromagnetic*, and thus cannot be a source of polarized spins, this large P is generated clearly by spin filtering in the EuS barrier. Polarization as high as 85% was found for a Al/3.3 nm EuS/Al superconductor–superconductor tunnel junction [25].

The temperature dependence of the junction resistance (R_J) also showed the spin-filtering effect of the EuS barrier. As expected for a tunnel junction with a semiconducting barrier, R_J increases as the temperature decreases. When the temperature decreases below the T_C of EuS, lowering of the tunnel barrier height for spin-up electrons due to exchange splitting of the conduction band results in a significant decrease of R_J with decreasing temperature. Spin polarization of the tunnel current was determined by another method: the barrier height Φ_0 was estimated by applying either the Brinkman [24] or Simmons [23] relation to the current–voltage characteristics of the junction for $T > T_C$, then $R_J(T)$ was used to quantify the amount of exchange splitting for $T < T_C$, and equation (3) to calculate P. This approach to quantifying P assumes no spin scattering. P values obtained using the latter method were in agreement with those obtained via the Meservey–Tedrow technique for EuS junctions [25]. R_J dropped as much as 65% from its maximum value at $T \sim T_C$.

Thin films of EuS, EuSe and EuO grown were polycrystalline, having saturation magnetization close to their bulk values even at thicknesses down to say 2 nm. For EuS bulk T_C was maintained in this thickness range, whereas by ∼1 nm thickness the T_C came down to ∼10 K. Because the magnetic moment of Eu^{2+} is rather high, between 7 and 8 μ_B, the magnetic properties of ultrathin EuX films can be easily measured using a SQUID magnetometer.

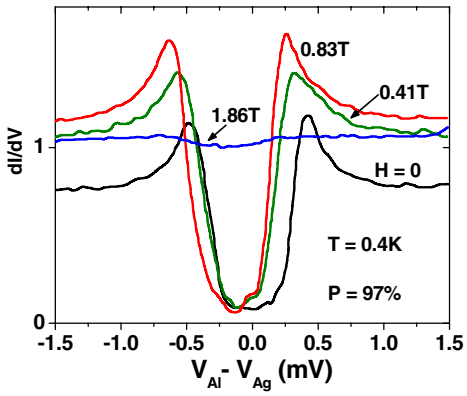

Figure 6. Conductance versus voltage for a Ag/EuSe/Al junction at 0.4 K taken at various applied magnetic fields. Note the highly symmetric curve at $H = 0$ whereas the peaks shift to lower energy corresponding to Zeeman energy as H increases. The polarization of the tunnel current is nearly 100%.

5.2. EuSe

The spin-filter behaviour of EuSe is quite different from that of EuS, because EuSe is an antiferromagnet at zero field. However, EuSe has an interesting magnetic phase diagram [52] such that it changes from the antiferromagnetic state into a ferrimagnetic state at low field or a ferromagnetic state at high field. Thus in an applied field, exchange splitting develops in the EuSe conduction band which increases as H_{appl} increases. This results in spin polarization of the tunnelling current, which increases as H_{appl} increases, or in other words, P becomes a function of H_{appl}. For the Ag/EuSe/Al tunnel junction shown in figure 6 at 0.4 K and $H_{\text{appl}} = 0$, the EuSe was in the antiferromagnetic state. Thus no Zeeman splitting was observed and the conductance was symmetric about $V = 0$. As H_{appl} increased and EuSe entered the ferromagnetic state, the polarization also increased. One also observes increasing Zeeman splitting and asymmetry as H_{appl} increased. Even in this case, the Zeeman splitting is much higher than the applied field as with the EuS barrier. The increasing asymmetry means an increased value of P. These effects are shown in figure 6. In fact, with optimum interface, P even reached as high as $97 \pm 3\%$, appearing as only one peak on either side of $V = 0$. *This is the first demonstration of a fully polarized tunnel current in a tunnel junction.* As seen in the $\mathrm{d}I/\mathrm{d}V$ curve for a junction of nearly 100% spin polarization, Zeeman splitting causes the two conductance peaks to shift to lower voltage (towards $V = 0$ on the positive side and becoming more negative on the reverse bias side). These two peaks correspond to the spin-up quasiparticle DOS, whereas the spin-down DOS have nearly zero conductance and thus are not seen in the $\mathrm{d}I/\mathrm{d}V$ curve.

In addition to a drop in R_{J} as the temperature decreases below T_{C} in an applied field, more interesting in the case of EuSe is a significant drop in R_{J} with increasing magnetic field, shown in figure 7(a). This decrease in R_{J} with increasing applied field results from the lowering of the spin-up barrier height as the field is applied, as shown schematically in figure 7(b). At zero field, EuSe is in the antiferromagnetic state. When a field is applied, EuSe changes into the ferromagnetic state and the conduction band undergoes exchange splitting, reaching a constant value at $\sim$1 T in this junction. This decrease in R_{J} can also be seen in figure 6 by the corresponding increase in conductance which, when translated to magnetoresistance, results in a value as high as 400%. *This is the first observation of resistance change in an applied field*

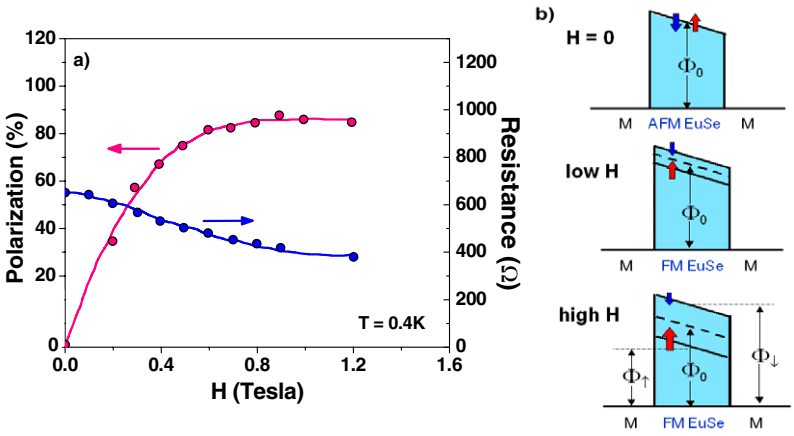

Figure 7. (a) Polarization and junction resistance as a function of applied field for a EuSe junction. (b) Schematic diagram of exchange splitting of the EuSe conduction band causing a change in spin-dependent barrier height with an applied field, to explain the behaviour shown in (a). At zero field, the barrier height is the same for both spin orientations (no exchange splitting). As the field increases, exchange splitting of the conduction band appears and increases, lowering the barrier height for spin-up electrons and raising it for spin-down electrons, giving rise to increasing P.

of such magnitude in a tunnel junction. Not only does R_J decrease with increasing field, but the spin-filter efficiency also improves as the amount of exchange splitting increases, resulting in increasing P until a constant value is reached (figure 7(a)). This dependence of polarization on applied magnetic field is unique to the EuSe spin filter. The question arises as to if $P = 0$ at zero applied field (the antiferromagnetic state of EuSe), as the model in figure 7(b) suggests. To answer this question, a EuS *underlayer* was employed to induce Zeeman splitting of Al at zero applied field in a EuS/Al/EuSe/Ag junction where again EuSe is the tunnel barrier. By use of such a structure, it was confirmed that EuSe does not filter spins at zero field, and indeed $P = 0$.

5.3. EuO

As mentioned earlier, stoichiometric EuO, as opposed to the more stable and nonferromagnetic Eu_2O_3, is quite difficult to grow at the monolayer scale necessary for tunnelling. Therefore demonstrating spin-filter tunnelling with a EuO barrier is much more challenging than for EuS and EuSe. With careful control of the film deposition parameters good quality EuO was grown in a Al/EuO/Y/Al tunnel junction, showing 29% polarization (figure 8). Similar to EuS and EuSe barriers, EuO showed a large enhancement of Zeeman splitting, amounting to an effective magnetic field of 3.9 T in a small applied field of just 0.1 T. Thus, the strong ferromagnetic order even in a 1.4 nm ultrathin film of EuO barrier created a large internal exchange field of 3.8 T. Zeeman splitting was observed at zero applied field as well. The exchange interaction of the EuO/Al bilayer had been observed in an earlier tunnelling study as well [53]. Even though EuO has a larger $2\Delta E_{ex}$ than EuS, which should result in a higher P, the spin-filtering efficiency of EuO is not as high. This was explained as due to the likely presence of defects at the EuO/electrode interfaces, caused by nonstoichiometry, which is quite difficult to control during sample growth. Yttrium was found to be the favourable electrode material to use with EuO, instead of for example Ag with which a lower $P = 9\%$ was obtained. Yttrium prevented over-oxidation of EuO into the undesirable Eu_2O_3. Confirmation of this came from study of the

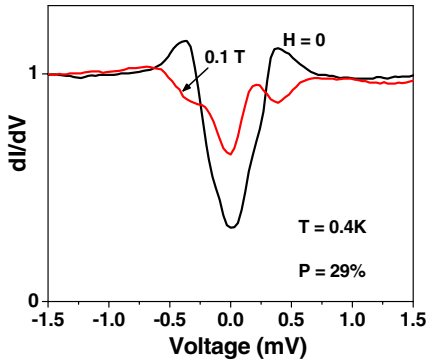

Figure 8. $\mathrm{d}I/\mathrm{d}V$ at 0.4 K for a Al/EuO/Y tunnel junction, showing 29% spin polarization. Asymmetry and Zeeman splitting can be seen at zero applied field.

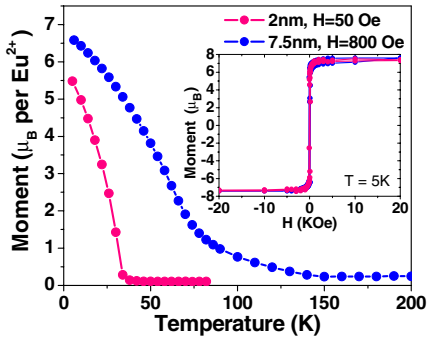

Figure 9. $M(H)$ (shown in the inset) and $M(T)$ for 2 nm and 7.5 nm EuO thin films. The 7.5 nm film shows bulk-like properties with $T_C = 69$ K. The 2 nm film shows a high moment, but a reduced $T_C = 35$ K.

chemical nature of the EuO interface with Y and Ag capping layers: this was examined using x-ray absorption spectroscopy and was found to agree with the tunnelling result [54].

Aside from a larger $2\Delta E_{ex}$, an advantage of EuO is that T_C is much higher, and thus spin filtering can be observed at higher temperatures. An interesting observation while studying these ultrathin EuO films was a reduction in the Curie temperature from the bulk value of EuO for monolayer thicknesses. Figure 9 compares the magnetization versus field behaviour and Curie temperature for a 7.5 nm film, showing bulk-like properties, and that for a 2 nm film. While the 2 nm film has the same saturation magnetization (7.4 μ_B per Eu^{2+} ion) as the thicker film, it has a T_C of 35 K, which is lower than the bulk $T_C = 69.3$ K.

5.4. Ferromagnetic insulator/superconductor exchange interaction with Eu chalcogenides

The enhanced Zeeman splitting of the Al superconducting DOS was observed for all EuS, EuSe and EuO low-temperature spin-polarized tunnelling measurements described above. This phenomenon is unique to thin film ferromagnetic insulator/superconductor (FMI/SC) systems and is elegantly observed by these experiments. Sarma [55] and de Gennes [56] had predicted this phenomenon 40 years ago as an exchange interaction between the ferromagnetically ordered ions in the FMI and the conduction electrons of the SC, which is analogous to a thin film superconductor in a uniform exchange field, schematically shown in the inset of

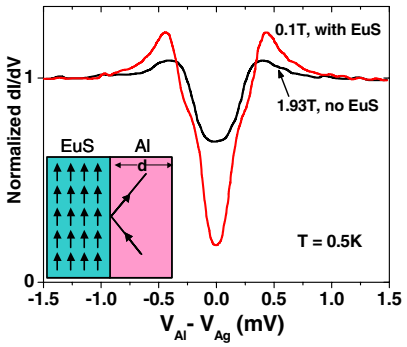

Figure 10. Normalized $\mathrm{d}I/\mathrm{d}V$ for a $Al/Al_2O_3/Ag$ junction in $H_{appl} = 1.93$ T, showing the broadening effect of orbital depairing, compared with a $EuS/Al/Al_2O_3/Ag$ junction, which shows enhanced Zeeman splitting in a small applied field of 0.1 T and an internal field of 1.8 T, with minimal orbital depairing. Inset: schematic diagram of the interaction between the Al quasiparticles during conduction with the ferromagnetically ordered ions in the EuS, at the FMI/SC interface.

figure 10. Because the thickness d of the superconducting film is small, boundary scattering of Al quasiparticles at the EuS/Al interface is dominant during conduction, where they exchange interact with the ordered Eu^{2+} ions. The resulting exchange field acts solely on the electron spins, and not on electron motion [55, 56]. Thus it causes Zeeman splitting, which is a spin effect, and has a negligible effect on orbital depairing in the SC. As an additional consequence of a purely field–spin interaction, when the critical field of the SC is reached, the phase transition to the normal state occurs through a first-order phase transition. de Gennes predicted that the magnitude of the field is inversely proportional to d, when d is less than the superconducting coherence length ξ. These predictions were experimentally verified [57] using the tunnel junction structure $EuS/Al/Al_2O_3/Ag$. The Al long electrode had a EuS layer under half of the strip whereas the other half had no EuS underlayer. The conductance of the junctions for the two configurations was compared; see figure 10. For the $EuS/Al/Al_2O_3/Ag$ configuration, enhanced Zeeman splitting, corresponding to a field of 1.9 T, was observed at $H_{appl} = 0.1$ T, whereas without EuS, for the $Al/Al_2O_3/Ag$ configuration, the same amount of Zeeman splitting is observed only with $H_{appl} = 1.93$ T. Furthermore, for the control junction a much higher conductance at zero bias and broadening of the peaks is observed, showing significant orbital depairing. This is not the case for junctions with EuS. It was also shown in this study that the superconducting Al film was driven normal by the internal field via a first-order transition, and the saturation internal field was inversely proportional to Al thickness. Furthermore, it was demonstrated that the exchange interaction only occurs for an FMI and SC in immediate proximity to each other. For example, the effect was lost when a thin layer of Al_2O_3, even just two monolayers, was inserted at the FMI/SC interface.

6. Quasimagnetic tunnel junctions

An alternative way of observing spin filtering is by measuring the tunnel magnetoresistance (TMR) in a quasimagnetic tunnel junction (QMTJ). By using the spin-filter material as the tunnel barrier between a normal (nonmagnetic) electrode (NM) and a ferromagnetic electrode of known polarization (P_{FM}), the spin-filter efficiency (P_{SF}) can be calculated from the TMR measurement by using Julliere's formula [58]:

$$\mathrm{TMR} = \frac{\Delta R}{R} = \frac{2P_{FM}P_{SF}}{(1 + P_{FM}P_{SF})}. \tag{4}$$

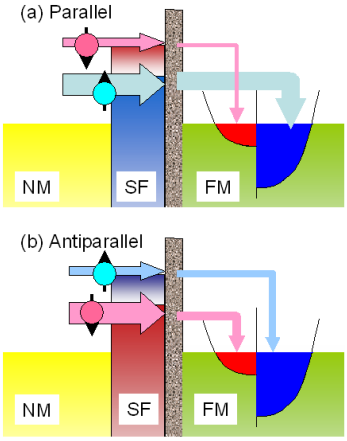

Figure 11. (a) Low resistance state for a QMTJ, with parallel alignment of magnetization of the spin-filter barrier (SF) and ferromagnetic electrode. (b) High resistance state for antiparallel alignment. In some junction structures, there is a very thin, nonmagnetic, insulating layer between the SF and FM, shown here, in order to prevent magnetic coupling between them.

The resistance (R_J) of the junction depends on the relative alignment of the magnetization of the spin-filter barrier and the ferromagnetic electrode—low resistance for parallel alignment (figure 11(a)) and high resistance for antiparallel alignment (figure 11(b)). Sharp, independent switching with well-separated coercivities for the two layers is necessary for observing TMR and quantifying P_{SF}. The trick to this approach is avoiding a magnetic coupling between the spin-filter barrier and the ferromagnetic electrode.

The high spin polarization (∼85%) found for EuS spin-filter barriers motivated further study of EuS in magnetic tunnel junctions [25]. For example, in the author's laboratory (at MIT) preliminary studies of Co/EuS/Al junctions gave a magnetoresistance (MR) ∼30% at 4.2 K for an applied field of 4 kOe, and an MR of 10% persisted even up to a bias of 2 V [59]. It was also observed that Co and EuS layers were antiferromagnetically coupled. LeClair *et al* [60] measured an MR $>$ 100% at 2 K for a QMTJ with a 5 nm EuS barrier sandwiched between Al and Gd electrodes, shown in figure 12. As can be seen in the measurement, there was considerable noise in the MR signal, which was attributed to instabilities in the EuS magnetization. The TMR decreased as the temperature was raised closer to the T_C of EuS (16 K). No MR was observed above the T_C. As expected for junctions with spin-filter barriers, a clear decrease of junction resistance was observed for these QMTJs when cooling below T_C, due to the lowering of the barrier height, as described earlier.

Recent results of our investigation of QMTJs of the structure Al/EuS/AlO_x/Co/CoO is mentioned below. The AlO_x layer between the EuS barrier and the Co electrode magnetically separates the layers, and the antiferromagnetic CoO acting as the exchange biasing layer pins the magnetization of the Co layer. Figure 13 shows the MR curve of the junction at 4.2 K taken with a bias of 5 mV. The shape of the MR curve is significantly improved, compared to the earlier work on EuS junction in figure 12. There is no instability in junction resistance, contrary to that seen by LeClair *et al* and in the case of $BiMnO_3$ and $NiFe_2O_4$ junctions described next.

The spin-filtering efficiency of perovskite $BiMnO_3$ [30] and ferrite $NiFe_2O_4$ [31] has been found using the QMTJ approach, using the half-metal $La_{2/3}Sr_{1/3}MO_3$ (LSMO) as the ferromagnetic electrode and ∼1 nm $SrTiO_3$ (STO) to magnetically decouple the LSMO and spin-filter layers. In the case of $BiMnO_3$ with an LSMO/STO/$BiMnO_3$/Au junction (figure 14(a)), a TMR of 29% at 3 K has been reported which dropped significantly with

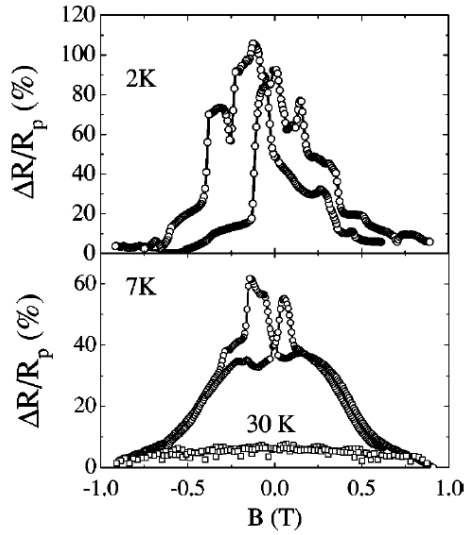

Figure 12. TMR > 100% of a QMTJ with a EuS barrier. Figure from [60].

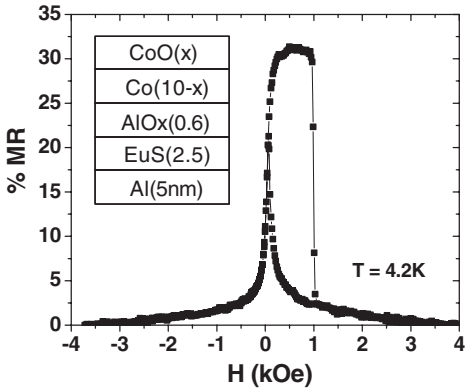

Figure 13. Magnetoresistance of Al/EuS/AlO_x/Co/CoO junction at 4.2 K at 5 mV.

increasing temperature. TMR vanished for $T > 40$ K, which is well below the bulk T_C (105 K) of $BiMnO_3$. This early disappearance of TMR may be due to the decreasing coercivity of $BiMnO_3$ as the temperature increases (as was observed in their measurement, figure 14(a)) or reduction of T_C from the bulk value for ultrathin films of $BiMnO_3$. The magnetic moment for their thin films reached only half the saturation magnetization of the bulk (moment of bulk $= 3.6\ \mu_B$/f.u.). Furthermore, in this single-crystalline layer $BiMnO_3$, Bi vacancies if present can disrupt the orbital ordering that determines the ferromagnetic interaction in $BiMnO_3$ and thus reduces T_C. The highest TMR observed for $BiMnO_3$ barriers in their study was 50%. Using equation (4) and assuming $P = 90\%$ for LSMO, this corresponded to a spin-filter efficiency of 22%. This positive value agrees with the band structure of $BiMnO_3$—lower barrier height for spin-up electrons. Contrary to the expected R_J versus T behaviour for a spin filter, the $BiMnO_3$ junctions did not show a decrease in R_J as T decreased, and instead showed increasing R_J with decreasing T (figure 14(a)). Adding 10% La to form a $LaBiMnO_3$

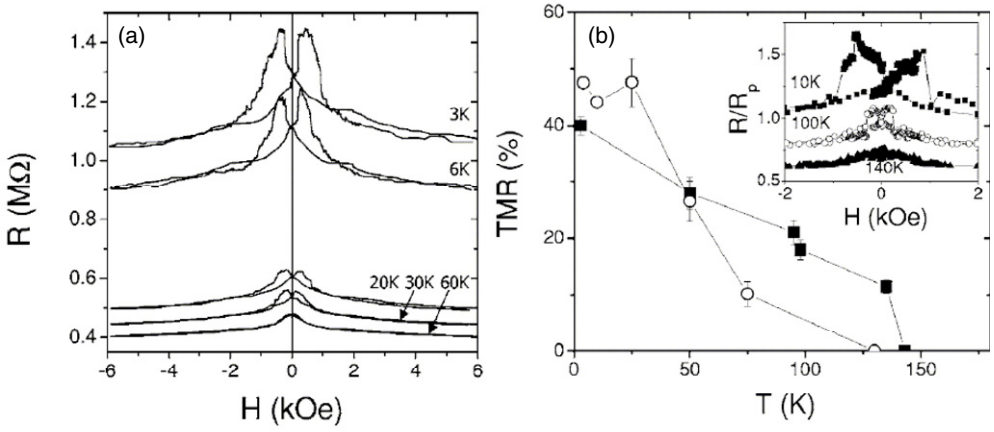

Figure 14. (a) Resistance as a function of field for a Au/3.5 nm $BiMnO_3$/1 nm STO/LSMO junction with a 10 mV bias at the indicated temperatures. Observed TMR of 29% at 3 K decreases with increasing temperature. Figure from [30]. (b) TMR versus temperature for a LSMO/$NiFe_2O_4$/Au junction, with (circles) and without (squares) STO at the LSMO/$NiFe_2O_4$ interface. Inset: resistance versus field, normalized to the parallel state and offset for clarity, at the indicated temperatures for the junction without STO. Figure from [31].

(LBMO) tunnel barrier improved the spin-filter efficiency [61], from 22% for $BiMnO_3$ to 35% for LBMO. La enters the lattice substitutionally and is known to stabilize the perovskite phase. A TMR of 90% was observed for these junctions.

Tunnel junctions of the structure LSMO/STO/$NiFe_2O_4$/Au with ferrimagnetic spinel $NiFe_2O_4$ barriers were studied in a similar manner (figure 14(b)). $P_{SF} = 22\%$ was obtained for junctions with STO at the LSMO/$NiFe_2O_4$ interface whereas it slightly reduced to 19% for junctions without STO. Again, the disappearance of TMR at temperatures above 140 K, well below the $T_C = 850$ K, may be due to the decrease in coercivity of $NiFe_2O_4$ with increasing temperature or a reduced T_C of LSMO caused by nonstoichiometry at the LSMO/$NiFe_2O_4$ interface. In addition, any nonstoichiometry in the barrier or the interfaces would create states in the potential barrier, which can lead to spin scattering and/or direct tunnelling without spin filtering. This would become more prominent with increasing temperature and bias. In the TMR measurement shown in the inset of figure 14(b), instabilities of resistance in the antiparallel alignment state were observed, as was the case for the MTJ of LeClair *et al* with EuS barriers described earlier. These instabilities were attributed to domains and domain wall structure in the $NiFe_2O_4$ film [31].

The positive sign of P_{sf} found for $NiFe_2O_4$ in this study is contrary to the band structure calculations [62] for $NiFe_2O_4$. Exchange splitting of the conduction band is such that the barrier height for *spin-down electrons is lower*, and thus a negative spin-filter efficiency is expected. The origin of this discrepancy is not understood.

Very recently, apparent spin filtering at room temperature using a ferrimagnetic $CoFe_2O_4$ spin filter was reported [63]. In this study, polarization of the tunnel current was deduced from the current–voltage behaviour of a $CoFe_2O_4$/$MgAl_2O_4$/Fe_3O_4 multilayer stack, for both parallel and antiparallel magnetization orientations of the $CoFe_2O_4$ and Fe_3O_4 layers, measured using a conducting atomic force microscope tip. More work needs to be done in order to confirm observation of spin filtering in this material.

Aside from the experimental demonstrations of TMR in the FM/spin filter/metal junctions just described, the theoretical work of Worledge and Geballe [64] predicts a TMR as high

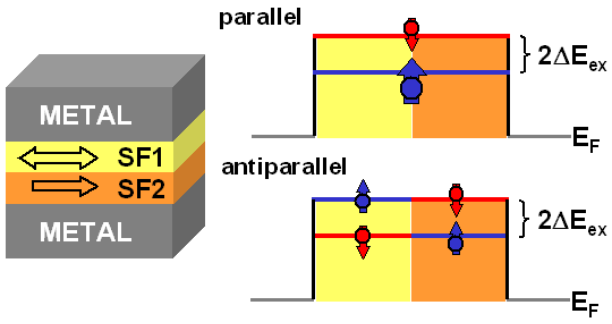

Figure 15. Schematic diagram of the double spin-filter junction proposed by Worledge and Geballe [64]. The magnetization of one spin filter (SF1) is free to switch in a small applied field while the other (SF2) is effectively pinned. The spin-up (blue) and spin-down (red) barrier heights for the two spin filters are shown for the parallel and antiparallel alignment. In this schematic diagram the two SF barriers are assumed to have identical band properties.

as 10^5 in a metal/spin filter 1/spin filter 2/metal structure called a double spin-filter junction (figure 15(a)). When the two spin-filter layers are magnetized parallel to each other, the spin-up electrons have a low barrier height and the spin-down electrons have a high barrier height, and thus a highly polarized spin-up current results. When the spin filters are magnetized antiparallel, the spin-up and spin-down barrier heights are mismatched so that very little current can flow (figure 15(b)). The independent, magnetic switching of the spin filters is achieved in this model by having spin filters with different, well-separated coercive fields, so that one spin filter is effectively pinned and the other is free to switch with applied field. According to this model, as one can expect, the exponential dependence of the tunnel current can yield exceedingly large MR by changing the relative magnetic alignment of the two spin filters. One major difficulty with this proposed device structure is its very high resistance. Due to the exponential dependence of junction resistance on barrier thickness (equation (2)), R_J will be much higher compared to the single spin-filter junctions. In the case of two different spin-filter materials with different band gaps and exchange splitting, an additional potential barrier could result from this heterojunction. Even more complicating is preventing coupling between two ferromagnetic spin filters so that parallel and antiparallel alignment can occur. Proposed double spin-filter devices with a similar operating principle, but with a nonmagnetic layer separating the spin filters, will be described in a later section.

7. Other approaches to spin filtering

7.1. Using quantum well states in nonmagnetic material

Using quantum well (QW) states is another approach to realize spin filtering. In a ferromagnetic material, energy levels of QW states depend on spin due to the exchange splitting, meaning that energy level of QW states for up-spin electrons will be different from that of down-spin electrons. This splitting of QW states enables one to select the resonant condition for each spin by applying the right bias voltage.

Such a type of spin-filtering scheme was reported by Slobodskyy *et al* [65] in 2003. They fabricated double barrier junctions of ZnSe/ZnBeSe/ZnMnSe/ZnBeSe/ZnSe and measured the I–V characteristics, as shown in figure 16. The ZnBeSe layers are tunnel barriers and the QW states are formed in a ZnMnSe layer which, although it is not ferromagnetic material, shows giant Zeeman splitting of the QW states in a magnetic field. The amount of splitting

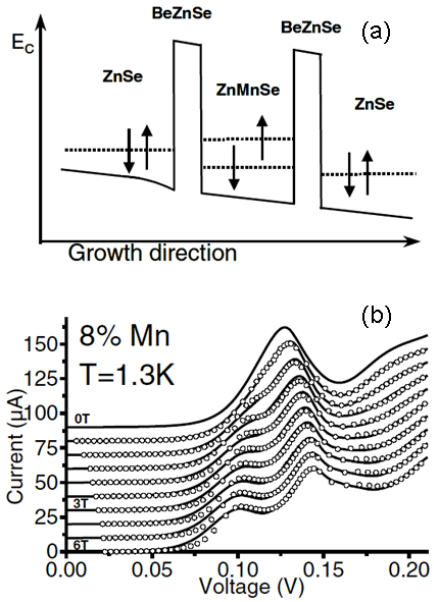

Figure 16. (a) Schematic view of the band diagram for a resonant tunnel junction under bias voltage. (b) I–V curves for a resonant tunnel junction in various magnetic fields. Figure from [65].

is controlled by the strength of the applied magnetic field. Figure 16(b) shows the I–V characteristics of their junctions in various magnetic fields. In zero field, a large resonant peak is observed at 0.12 V. The peak splits into two peaks in an applied magnetic field, and the width of splitting increases with magnetic fields, corresponding to the giant Zeeman splitting. Each of two peaks can be attributed to up-spin and down-spin QW states. Under this condition one can select the desired spin current by applying proper bias voltage to the structure.

7.2. Spin filtering by using the Rashba effect

In the section above, the magnetic materials are necessary in the junctions to create spin filtering. In a totally different approach, a spin filter which does not need a magnetic material is proposed by Koga *et al* [66]. According to their model, the Rashba spin–orbit coupling effect (Rashba effect [67]) is expected to induce spin-split resonant tunnelling levels in the devices. The device has three tunnel barriers and two quantum wells. The feature of the device is the 'mountain-like potential' shown in figure 17. This characteristic potential may be realized by using InGaAs and InAlAs with proper parameters, i.e. thickness, impurity densities and so on.

According to Koga *et al*, the one-dimensional Hamiltonian in the potential is written as follows,

$$\begin{aligned} &\frac{\hbar^2 k_z^2}{2m^*(z)} + U^{\mathrm{eff}}_{\uparrow,\downarrow}(\mathbf{k}_\parallel, z) = E_z, \\ &U^{\mathrm{eff}}_{\uparrow,\downarrow}(\mathbf{k}_\parallel, z) = \frac{\hbar^2 k_\parallel^2}{2m^*(z)} \pm \alpha(z) k_\parallel + U_0(z) - E_{\mathbf{k}\parallel}, \end{aligned} \tag{5}$$

where m^* is the effective mass of an electron, the z-axis is perpendicular to the tunnel barrier, $k_\parallel$ is the parallel momentum component, and $\alpha(z)$ is the Rashba constant at position z. The plus and minus sign of $\alpha(z)$ correspond to the Hamiltonian for up-spin and down-spin electrons.

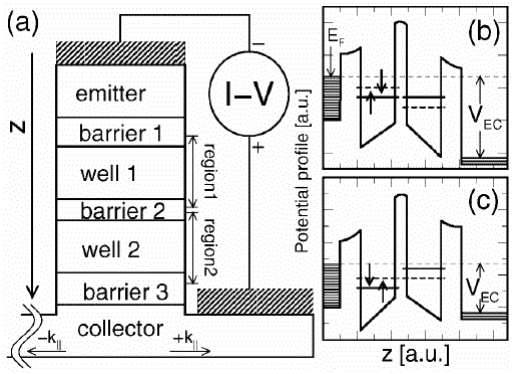

Figure 17. (a) Schematic illustration of the proposed spin-filter device. ((b), (c)) Conduction band potential profiles for the proposed device. The solid lines and broken line are QW states for up-spin and down-spin electrons respectively. Figure from [66].

This Hamiltonian results in a spin-dependent energy level of quantum well states. Therefore this device can show spin selectivity of the resonant tunnel current.

As described in this section, spin filtering using quantum well states has some attractive characteristics: (1) one can select the spin by applying a bias voltage, (2) the voltage is controlled easily by the width of quantum well structure. On the other hand, creating device structures with appropriate materials and high quality of films are necessary to realize this.

8. Spin injection into semiconductors

Successful experimental demonstration of spin filtering in a tunnel barrier led the way to a theoretical proposal of semiconductor spin-filter transistor (SFT) device by Sugahara and Tanaka [68]. This proposed device consists of a nonmagnetic, semiconducting emitter, base and collector separated by two spin-filter tunnel barriers. The emitter barrier filters the spins of hot electrons as they tunnel from the emitter into the base when an emitter–base bias is applied, allowing only spin-up electrons into the base. The collector barrier acts as a spin analyser for the spin-polarized transport through the base. The width of the base must be less than the spin-flip scattering length. When the spin-filter barriers are magnetized parallel to each other, as in figure 18(a), the spin-up electrons injected into the base can tunnel through the collector barrier (lower barrier height for spin-up electrons), and a highly polarized collector current will be detected. When the spin-filter barriers are magnetized in an antiparallel configuration, as in figure 18(b), the spin-up electrons injected into the base cannot tunnel across the too high collector barrier, and hardly any collector current is detected. Hence, the magnetization configuration of the emitter and collector tunnel barriers determines the output of the SFT; the collector current for parallel configuration can be significantly higher than that for antiparallel configuration. Key parameters include tunnel barrier height and the amount of exchange splitting in the spin filters, mean free path of hot electrons in the base layer, thickness of the two spin-filter barriers (W_{EB} and W_{BC}), and width of the base W_B. From the calculated I–V characteristics of their device, Sugahara *et al* showed that the SFT could achieve large magneto-current ratio, current gain, and power gain.

Filip *et al* [69] proposed a similar device, consisting of two EuS spin-filter tunnel barriers separated by a nonmagnetic semiconducting quantum well. The spin injection device was modelled using the EuS/PbS system because it can be grown epitaxially and also due to the

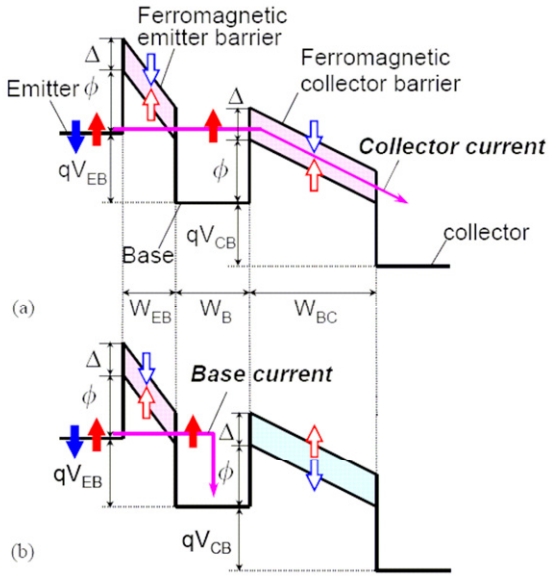

Figure 18. Schematic diagram of the spin-filter transistor proposed by Sugahara and Tanaka. (a) Parallel magnetic orientation of the emitter barrier and collector barrier, resulting in a high collector current. (b) Antiparallel magnetic orientation, resulting in no collector current. Figure from [68].

high spin-filter efficiency of EuS. In addition, antiparallel magnetization alignment of the two EuS layers may be easier to obtain due to antiferromagnetic interlayer exchange coupling for the EuS/PbS/EuS trilayer [70]. According to this model, when the EuS layers are aligned antiparallel, a nonequilibrium spin accumulation takes place in the PbS quantum well. No spin accumulation takes place when they are aligned parallel. Calculation shows that this can result in high magnetoresistance for a range of EuS and PbS layer thicknesses.

Experimental work integrating spin filters with semiconductors for injection and detection of highly spin-polarized currents has a long way to go before catching up with theoretical models. Initial steps to reach the goal include a study the metal/EuS Schottky contact [71] and EuS/GaAs semiconductor heterojunction [72]. For the metal/EuS Schottky contact (100 nm thick EuS layer), exchange splitting of the EuS conduction band was determined by measuring the I–V characteristics at temperatures above and below the T_C of EuS, and then extracting (from forward bias I–V) the change in Schottky barrier height as it lowers for $T < T_C$. Exchange splitting caused lowering of the barrier height. For the EuS/GaAs heterojunction, exchange splitting of 0.48 eV (much higher than previously observed values in optical studies [33] and tunnelling studies [25]) was found in a similar manner from the forward bias I–V (electron injection from EuS into GaAs). In addition, a shift of the I–V characteristics with temperature was observed in reverse bias (injection from GaAs into EuS), suggesting filtering of the unpolarized electrons coming from GaAs. In this way, the performance of the EuS/GaAs heterojunction as an injector and detector was probed individually. The observed shifts in the I–V characteristics with temperature, caused by exchange splitting of the EuS conduction band, implied spin-polarized injection and detection, though no spin analyser was explicitly used.

Many of quantum computers proposed so far use an electron spin as a qubit. There are theoretical proposals about quantum computing using a spin filter. Spin-filter tunnelling

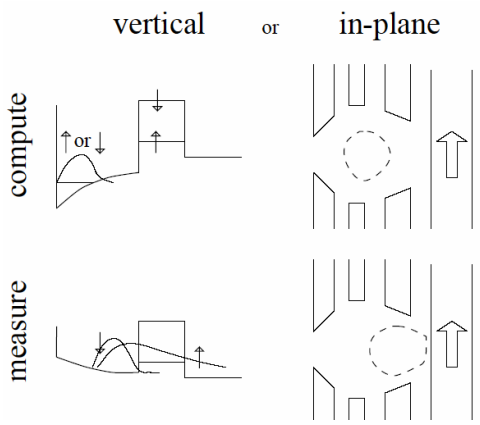

Figure 19. Schematic illustrations of the spin-filter quantum measurement. Possible vertical and in-plane structures are shown. In the computing phase the electron wavefunction in the quantum dot is held far from the ferromagnetic spin filter. In the measure phase the gate potentials are changed so that the electron wavefunction is pressed up against the spin filter. Figure from [73].

is being thought of as one of the ways to achieve quantum computing [73, 74], as shown schematically in figure 19. In this scheme the spin-filter property of the barrier provides the method for the quantum measurement. Here the correlation of the electron wavefunction from one quantum dot to the adjacent one is by spin tunnelling through the spin selective barrier. The energy level of the trapped electron is varied by an applied gate voltage, allowing it to tunnel or not through the barrier placed beside a quantum dot. The tunnelling probability depends on the magnetization orientation of the spin-filter barrier and hence the spin state of the trapped electron can be read, allowing measurement of the state of each qubit individually and reliably by electrical means rather than the extremely difficult task of magnetically measuring a single spin. Thus spin information is converted into charge information. This is a very simple way, although there are many material and parameters which must be investigated to reach the goal. Other group proposed a spin filter and a spin memory using quantum dots. It is realized by the quantum dots in the Coulomb blockade regime in a magnetic field [75].

9. Conclusion

The spin-filtering phenomenon is certainly quite fascinating, especially with europium compounds, showing very interesting physics. As is seen, most of the effects originate within a few monolayer levels of the materials or at an interfacial interaction with a superconductor. One can study ferromagnetic behaviour in these magnetic semiconductors down to the monolayer level by tunnelling. Large internal exchange fields available can be utilized to study the physics in systems where application of an external field may not be suitable. Generating a nearly fully polarized beam of electrons is an extremely useful tool for fundamental studies as well as for application in the emerging field of spintronics, especially for spin injection/detection in semiconductors. For instance, one can inject highly polarized spins into say Si or GaAs either from doped magnetic semiconductors or using the doped magnetic semiconductor as a barrier. A similar scheme can be adopted for detection as well.

Although growing ultrathin films of Eu chalcogenide compounds is relatively easy (except for EuO), they work only at low temperature, as the magnetic ordering temperatures are low. One way to escape from this issue is to use ferrites, which have T_C above room temperature. However, understanding and controlling the structure, stoichiometry and the

magnetic properties of ultrathin layers of complex oxides is extremely challenging. The interfacial compatibility and bond-driven, intrinsic magnetic behaviour can be different from what one expects for the ferrites. All these problems have to be solved before one can realize their potential. It is encouraging to see that good progress is being made in this direction [76, 77, 31].

Acknowledgments

We would like to thank Dr R Meservey for his deep interest in this work over the years. For many years NSF and ONR funds have supported this work. In the recent times funding from the KIST-MIT joint project and CMI funds at MIT have supported the program.

References

[1] Merzbacher E 2002 The early history of quantum tunnelling *Phys. Today* **55** 44
[2] Giaever I 1960 Energy gap in superconductors measured by electron tunnelling *Phys. Rev. Lett.* **5** 147
Giaever I 1960 Electron tunnelling between two superconductors *Phys. Rev. Lett.* **5** 464
[3] Bardeen J, Cooper L N and Schrieffer J R 1957 Theory of superconductivity *Phys. Rev.* **108** 1175
[4] Meservey R, Tedrow P M and Fulde P 1970 Magnetic field splitting of the quasiparticle states in superconducting aluminum films *Phys. Rev. Lett.* **25** 1270
[5] Tedrow P M and Meservey R 1971 Spin-dependent tunnelling into ferromagnetic nickel *Phys. Rev. Lett.* **26** 192
Tedrow P M and Meservey R 1973 Spin polarizations of electron tunnelling from films of Fe, Co, Ni and Gd *Phys. Rev.* B **7** 318
[6] Meservey R and Tedrow P M 1994 Spin-polarized electron tunnelling *Phys. Rep.* **238** 173
[7] Moodera J S, Nassar J and Mathon G 1999 Spin-tunnelling in ferromagnetic junctions *Annu. Rev. Mater. Sci.* **29** 381
[8] Gregg J F, Petej I, Jouguelet I E and Dennis C 2002 Spin electronics—a review *J. Phys. D: Appl. Phys.* **35** R121
[9] Moodera J S and Meservey R 2004 Spin polarized tunneling *Magnetoelectronics* ed M Johnson (New York: Elsevier–Academic Press) chapter 3
[10] Maki K 1969 *Superconductivity* vol 2, ed R D Parks (New York: Dekker) p 1035
Fulde P and Maki K 1966 Theory of superconductor combining magnetic impurities *Phys. Rev.* **141** 275
[11] Stearns M B 1977 Simple explanation of tunnelling spin-polarization of Fe, Co, Ni and its alloys *J. Magn. Magn. Mater.* **5** 167
[12] Bardeen J 1961 Tunneling from many-particle point of view *Phys. Rev. Lett.* **6** 57
[13] Mazin I I 1999 How to define and calculate the degree of spin polarization in ferromagnets *Phys. Rev. Lett.* **83** 1427
[14] Tsymbal E Y and Pettifor D G 1997 Modelling of spin-polarized electron tunnelling from 3d ferromagnets *J. Phys.: Condens. Matter* **9** L411
Oleinik I I, Tsymbal E Y and Pettifor D G 2000 Structural and electronic properties of Co/Al_2O_3/Co magnetic tunnel junction from first principles *Phys. Rev.* B **62** 3952
[15] Gadzuk J W 1969 Band-structure effects in the field-induced tunnelling of electrons from metals *Phys. Rev.* **182** 416
Hertz J A and Aoi K 1973 Spin-dependent tunnelling from transition-metal ferromagnets *Phys. Rev.* B **8** 3252
[16] Moodera J S and Mathon G 1999 Spin polarized tunnelling in ferromagnetic junctions *J. Magn. Magn. Mater.* **200** 248
[17] de Groot R, Mueller F, van Engen P and Buschow K 1983 New class of materials: half-metallic ferromagnets *Phys. Rev. Lett.* **50** 2024
[18] Schwarz K 1986 CrO_2 predicted as a half-metallic ferromagnet *J. Phys. F: Met. Phys.* **16** L211
[19] Pickett W E and Singh D J 1996 Electronic structure and half-metallic transport in the $La_{1-x}Ca_xMnO_3$ system *Phys. Rev.* B **53** 1146
[20] Parker J S, Watts S M, Ivanov P G and Xiong P 2002 Spin polarization of CrO_2 at and across an artificial barrier *Phys. Rev. Lett.* **88** 196601
[21] Orgassa D, Fujiwara H, Schulthess T C and Butler W H 1999 First-principles calculation of the effect of atomic disorder on the electronic structure of the half-metallic ferromagnet NiMnSb *Phys. Rev.* B **60** 13237

de Wijs G A and de Groot R A 2001 Towards 100% spin polarized charge-injection: The half-metallic NiMnSb/CdS interface *Phys. Rev.* B **64** 020402
[22] Tanaka C, Nowak J and Moodera J S 1999 Spin-polarized tunnelling in a half-metallic ferromagnet *J. Appl. Phys.* **86** 6239
[23] Simmons J G 1963 Generalized formula for the electric tunnel effect between similar electrodes separated by a thin insulating film *J. Appl. Phys.* **34** 1793–803
[24] Brinkman W F, Dynes R C and Rowell J M 1970 Tunneling conductance of asymmetrical barriers *J. Appl. Phys.* **41** 1915–21
[25] Moodera J S, Hao X, Gibson G A and Meservey R 1988 Electron-spin polarization in tunnel junctions in zero applied field with ferromagnetic EuS barriers *Phys. Rev. Lett.* **61** 637–40
Hao X, Moodera J S and Meservey R 1990 Spin-filter effect of ferromagnetic europium sulfide tunnel barriers *Phys. Rev.* B **42** 8235–43
[26] Moodera J S, Meservey R and Hao X 1993 Variation of the electron-spin polarization in EuSe tunnel junctions from zero to near 100% in a magnetic field *Phys. Rev. Lett.* **70** 853–6
[27] Santos T S and Moodera J S 2004 Observation of spin filtering with a ferromagnetic EuO tunnel barrier *Phys. Rev.* B **69** 241203(R)
[28] Keller J, Parker J S, Stankiewicz J, Read D E, Stampe P A, Kennedy R J, Xiong P and von Molnár S 2002 Controlling the magneto-transport properties of EuS thin films *IEEE Trans. Magn.* **38** 2673–5
[29] Pénicaud M, Siberchicot B, Sommers C B and Kübler J 1992 Calculated electronic band structure and magnetic moments of ferrites *J. Magn. Magn. Mater.* **103** 212–20
[30] Gajek M, Bibes M, Barthélémy S, Bouzehouane K, Fusil S, Varela M, Fontcuberta J and Fert A 2005 Spin filtering through ferromagnetic $BiMnO_3$ tunnel barriers *Phys. Rev.* B **72** 020406(R)
[31] Lüders U, Bibes M, Bouzehouane K, Jacquet E, Contour J-P, Fusil S, Bobo J-F, Fontcuberta J, Barthélémy A and Fert A 2006 Spin filtering through ferrimagnetic $NiFe_2O_4$ tunnel barriers *Appl. Phys. Lett.* **88** 082505
[32] Hass C 1970 Magnetic Semiconductors *CRC Crit. Rev. Solid State Sci.* **1** 47–98
[33] Wachter P 1979 Europium chalcogenides: EuO, EuS, EuSe, and EuTe *Handbook on the Physics and Chemistry of Rare Earths* vol 2, ed K A Schneider and L Eyring (New York: North-Holland) pp 507–74
[34] Holtzberg F, von Molnar S and Coey J M D 1980 Rare earth magnetic semiconductors *Handbook on Semiconductors* vol 3, ed S P Keller (New York: North-Holland) pp 803–56
[35] Mauger A and Godart C 1986 The magnetic, optical, and transport properties of representatives of a class of magnetic semiconductors: the europium chalcogenides *Phys. Rep.* **141** 51–176
[36] Kulatov É T, Uspenskiĭ Y A and Khalilov S V 1996 Electronic structure and magnetooptical properties of europium monochalcogenides EuO and EuS *Phys. Solid State* **38** 1677–8
[37] Horne M, Strange P, Temmerman W M, Szotek Z, Svane A and Winter H 2004 The electronic structure of europium chalcogenides and pnictides *J. Phys.: Condens. Matter* **16** 5061–70
[38] Ghosh D B, De M and De S K 2004 Electronic structure and magneto-optical properties of magnetic semiconductors: europium monochalcogenides *Phys. Rev.* B **70** 115211
[39] Busch G, Junod P and Wachter P 1964 Optical absorption of ferro- and antiferromagnetic europium chalcogenides *Phys. Lett.* **12** 11–2
[40] Steeneken P G, Tjeng L H, Elfimov I, Sawatzky G A, Ghiringhelli G, Brookes N B and Huang D-J 2002 Exchange splitting and charge carrier spin polarization in EuO *Phys. Rev. Lett.* **88** 047201
[41] Shafer M W and McGuire T R 1968 Studies of Curie-point increases in EuO *J. Appl. Phys.* **39** 588
[42] Ott H, Heise S J, Sutarto R, Hu Z, Chang C F, Hsieh H H, Lin H-J, Chen C T and Tjeng L H 2006 Soft x-ray magnetic circular dichroism study on Gd-doped EuO thin films *Phys. Rev.* B **73** 094407
[43] Massenet O, Capiomont Y and Van Dang N 1974 Effects of high nonstoichiometry of EuO properties *J. Appl. Phys.* **45** 3593–9
[44] Schoenes J and Wachter P 1974 Exchange optics in Gd-doped EuO *Phys. Rev.* B **9** 3097–105
[45] Kasuya T and Yanase A 1968 Anomalous transport phenomena in Eu–chalcogenide alloys *Rev. Mod. Phys.* **40** 684
[46] Müller N, Eckstein W, Heiland W and Zinn W 1972 Electron spin polarization in field emission from EuS-coated tungsten tips *Phys. Rev. Lett.* **29** 1651–4
[47] Kisker E, Baum G, Mahan A H, Raith W and Schröder K 1976 Conduction-band tunnelling and electron-spin polarization in field emission from magnetically ordered europium sulfide on tungsten *Phys. Rev. Lett.* **36** 982–5
[48] Baum G, Kisker E, Mahan A H, Raith W and Reihl B 1977 Field emission of monoenergetic spin-polarized electrons *Appl. Phys.* **14** 149–53
[49] Kisker E, Baum G, Mahan A H, Raith W and Reihl B 1978 Electron field emission from ferromagnetic europium sulfide on tungsten *Phys. Rev.* B **18** 2256–75

[50] Esaki L, Stiles P J and von Molnar S 1967 Magnetointernal field emission in junctions of magnetic insulators *Phys. Rev. Lett.* **19** 852–4
[51] Thompson W A, Holtzberg W A, McGuire T R and Petrich G 1972 Tunneling study of EuS magnetization *Magnetism and Magnetic Materials: Proc. of the 17th Annual Conf. on Magnetism and Magnetic Materials (Chicago, 1971)* (*AIP Conf. Proc. No. 5*) ed C D Graham Jr and J J Rhyne (New York: AIP) pp 827–36
[52] Griessen R, Landolt M and Ott H R 1971 A new ferromagnetic phase in EuSe below 1.8 K *Solid State Commun.* **9** 2219–23
[53] Tedrow P M, Tkaczyk J E and Kumar A 1986 Spin-polarized electron tunnelling study of an artificially layered superconductor with internal magnetic field: EuO–Al *Phys. Rev. Lett.* **56** 1746
[54] Negusse E, Holroyd J, Liberati M, Dvorak J, Idzerda Y U, Santos T S, Moodera J S and Arenholz E 2006 Effect of electrode and EuO thickness on EuO–electrode interface in tunnelling spin filter *J. Appl. Phys.* **99** 08E507
[55] Sarma G 1963 On the influence of a uniform exchange field acting on the spins of the conduction electrons in a superconductor *J. Phys. Chem. Solids* **24** 1029–32
[56] de Gennes P G 1966 Coupling between ferromagnets through a superconducting layer *Phys. Lett.* **23** 10–1
[57] Hao X, Moodera J S and Meservey R 1991 Thin-film superconductor in an exchange field *Phys. Rev. Lett.* **67** 1342–5
Hao X 1990 The study of ferromagnetic EuS: The spin filter and proximity effects *PhD Thesis* MIT, Cambridge, USA, unpublished
[58] Julliere M 1975 Tunneling between ferromagnetic films *Phys. Lett.* A **54** 225–6
[59] Nasser J and Moodera J S 1998 unpublished data
[60] LeClair P, Ha J K, Swagten H J M, Kohlhepp J T, van de Vin C H and de Jonge W J M 2002 Large magnetoresistance using hybrid spin filter devices *Appl. Phys. Lett.* **80** 625–7
[61] Gajek M, Bibes M, Varela M, Fontcuberta J, Herranz G, Fusil S, Bouzehouane K, Barthélémy A and Fert A 2006 $La_{2/3}Sr_{1/3}MnO_3$—$La_{0.1}Bi_{0.9}MnO_3$ heterostructures for spin filtering *J. Appl. Phys.* **99** 08E504
[62] Szotek Z, Temmerman W M, Svane A, Petit L, Strange P, Stocks G M, Ködderitzsch D, Hergert W and Winter H 2004 Electronic structure of half-metallic ferromagnets and spin ferromagnetic insulators *J. Phys.: Condens. Matter* **16** S5587–600
[63] Chapline M G and Wang S X 2006 Room-temperature spin filtering in a $CoFe_2O_4/MgAl_2O_4/Fe_3O_4$ magnetic tunnel barrier *Phys. Rev.* B **74** 014418
[64] Worledge D C and Geballe T H 2000 Magnetoresistive double spin filter tunnel junction *J. Appl. Phys.* **88** 5277–9
[65] Slobodskyy A, Gould C, Slobodskyy T, Becker C R, Schmidt G and Molenkamp L M 2003 Voltage-controlled spin selection in a magnetic resonant tunnelling diode *Phys. Rev. Lett.* **90** 246601
[66] Koga T, Nitta J, Takayanagi H and Datta S 2002 Spin-filter device based on the Rashba effect using a nonmagnetic resonant tunnelling diode *Phys. Rev. Lett.* **88** 126601
[67] Rashba E I 1960 Properties of semiconductors with an extremum loop. Cyclotron and combinational resonance in a magnetic field perpendicular to the plane of the loop *Sov. Phys.—Solid State* **2** 1109–22
[68] Sugahara S and Tanaka M 2004 A novel spin transistor based on spin-filtering in ferromagnetic barriers: a spin-filter transistor *Physica* E **21** 996–1001
[69] Filip A T, LeClair P, Smits C J P, Kohlhepp J T, Swagten H J M, Koopmans B and de Jonge W J M 2002 Spin-injection device based on EuS magnetic tunnel barriers *Appl. Phys. Lett.* **81** 1815–7
[70] Smits C J P, Filip A T, Swagten H J M, Koopmans B and de Jonge W J M 2004 Antiferromagnetic interlayer exchange coupling in all-semiconducting EuS/PbS/EuS trilayer *Phys. Rev.* B **69** 224410
[71] Ren C, Trbovic J, Xiong P and von Molnár S 2005 Zeeman splitting in ferromagnetic Schottky barrier contacts based on doped EuS *Appl. Phys. Lett.* **86** 012501
[72] Trbovic J, Ren C, Xiong P and von Molnár S 2005 Spontaneous spin-filter effect across EuS/GaAs heterojunction *Appl. Phys. Lett.* **87** 082101
[73] DiVincenzo D P 1999 Quantum computing and single-qubit measurements using the spin-filter effect *J. Appl. Phys.* **85** 4785
[74] Bennett C H and DiVincenzo D P 2000 Quantum information and computation *Nature* **404** 247
[75] Recher P, Sukhorukov E V and Loss D 2000 Quantum dot as spin filter and spin memory *Phys. Rev. Lett.* **85** 1962–5
[76] Ramos A, Moussy J B and Gautier-Soyer M, unpublished
[77] Hu G, Choi J H, Eom C B, Harris V G and Suzuki Y 2000 Structural tuning of the magnetic behavior in spinel-structure ferrite thin films *Phys. Rev.* B **62** R779–82